Numerical Study on the Improvement of Resistance Performance for Fast-ferry with Transom Appendage

Chun-Beom Hong*, **Jung-Joong Kim**
Marine Research Institute, Samsung Heavy Industries Co., Daejeon 305-380, Korea

In recent, stern wedges and stern flaps are installed for the improvement of propulsion and resistance performance of fast-ferry. For example, U.S. Navy has achieved the development of stern wedges and stern flaps for destroyer to enhance powering performance. It is generally known that stern wave systems as well as bow wave systems play an important role in the wave making resistance performance for fast-ferry. The bow diverging wave system has been usually simulated by an interface tracking method (ITM). However, it is difficult to apply the ITM to the numerical simulation of the stern wave and spray phenomenon because of over-turning wave and wave-breaking. Therefore, to solve this problem an interface capturing method (ICM) is introduced. In the present study, a numerical method with the ICM is developed to evaluate the resistance performance of fast-ferry. Incompressible Navier-Stokes and continuity equations are employed in the present study and the equations are discretized by Finite Difference Method in the general curvilinear coordinate system. CIP (Constrained Interpolated Profile) method is used for the discretization of convection terms, respectively. The free surface location is determined by level set method. In order to validate the numerical method, numerical simulations for Wigley hull are performed and their results are compared with experimental results. Several numerical simulations of ship waves for fast-ferry are performed to find advantages of appendage installation. Through those simulations, the computed results, such as wave profile and resistance coefficient, are compared with the measured results which are achieved from Samsung Ship Model Basin (SSMB). The effects of transom appendage on the resistance performance are discussed with the computed results in this study.

Key Words : Propulsion and Resistance Performance, Fast-ferry, Finite Difference Method, Level Set Method, Constrained Interpolated Profile (CIP) Method

1. Introduction

Many concepts are available for ships to save fuel, or to increase speed, but these improvements are frequently high-cost, high-risk, or even require new vessels. On the other hand, the transom appendages are ingenious manipulation of flow around the hull, which produces tangible performance benefits with less cost and can be back-fit to a ship with little change to the hull. It is generally known that the powering benefit of principal transom appendage is attributable to the induced change in the flow field around the stern. These flow field changes cause a reduction of drag on the after hull, and improve the wave resistance of the ship. Karafiath et al.(1999) reported that the U.S. Navy has installed transom appendages on many vessels which exhibited significant fuel savings and maximum speed increases during sea trials.

* Corresponding Author,
E-mail : cb.hong@samsung.com
TEL : +82-42-865-4782; **FAX** : +82-42-865-4380
Marine Research Institute, Samsung Heavy Industries Co., Daejeon 305-380, Korea. (Manuscript **Received** November 28, 2005; **Revised** November 20, 2006)

In the present study, the simulation of free surface flow is highly necessary to find the reason for the improvement of resistance performance due to the transom wedge for a fast-ferry. The free surface flow is a difficult part of flows due to the moving boundary. The location of the free surface is a solution with known initial value and the boundary condition has a nonlinear property. Two kinds of free surface treatment have been broadly introduced. One is the interface tracking method (ITM), and the other is the interface capturing method (ICM). The ITM is useful for smooth flow since the height function of the interface is available for the determination of a unique solution corresponding to horizontal plane, and the computational time is relatively shorter than that of ICM. Hong et al.(2005) shows usefulness of ITM for the ship waves. However, it is impossible to adopt the ITM in the computation of violent free surface flow with multi-solution corresponding to horizontal plane. Therefore, the ICM is adopted for the numerical simulation of complex wave system. The ICM is suitable for the computation in the present study since the complex phenomena, such as spray and overturning wave near by bow and transom stern, are observed. The ICM is verified by computing the ship wave and its results are compared to those of ITM. The present numerical method is applied for the simulation of ship waves for fast-ferry cruising and the resistance performances for both with and without transom wedge are discussed.

Watanabe et al.(1999) showed good results in the propagated waves particularly. In this study, CIP method is applied to analyze the ship waves. The calculated waves by CIP method and MAC method were compared to discuss the computational resolution.

2. Governing Equations and Boundary Conditions

Three-dimensional incompressible Navier-Stokes and continuity equations are employed for the present study. The governing equations are expressed as following equations (1) and (2).

$$\frac{\partial \vec{v}}{\partial t}+(\vec{v}\cdot\nabla)\vec{v}=-\frac{\nabla p}{\rho}+\frac{\mu}{\rho}\nabla^2\vec{v}+\vec{F} \tag{1}$$

$$\nabla\cdot\vec{v}=0 \tag{2}$$

where $\vec{v}$ and t are velocity vector and time, respectively. $\vec{F}$ is the external force including gravitational force. The ρ and μ are density and viscosity, respectively.

The location of the interface using ICM is determined by a transport equation (3) for distance function while the free surface boundary condition as shown in equation (4) is set in ITM. On the upstream boundary of the computational domain, the uniform flow condition is applied, while zero gradient condition is given on the outer boundary. On the center plane, the symmetric boundary condition is applied.

$$\frac{\partial \varphi}{\partial t}+\vec{v}\cdot\nabla\varphi=0 \tag{3}$$

$$\frac{\partial \zeta}{\partial t}=w-u\frac{\partial \zeta}{\partial x}-v\frac{\partial \zeta}{\partial y} \tag{4}$$

3. Numerical Method

3.1 Interface capturing method

In order to simulate overturning wave around ships, Miyata et al.(1985, 1988) improved the Maker and Cell method and Kong et al.(2004) showed complex wave phenomena disturbed by sub-merged plated. The MAC method has been used widely because of its good applicability but the computing effort is large, since in addition to solving the equation governing fluid flow, one has to follow the motion of large number of particles. This is the reason why level set method proposed by Osher and Sethian (1988) was adopted in the present study. In order to prevent the numerical smearing of the distance function, the reinitialization of the distance function suggested by Sussman and Fatemi (1999) is introduced. The reinitialization guarantees the constant width of interface but violates the mass conservation because the variations of the distance function due to the reinitialization in each direction are not same. Therefore, an additional process is required to conserve the mass.

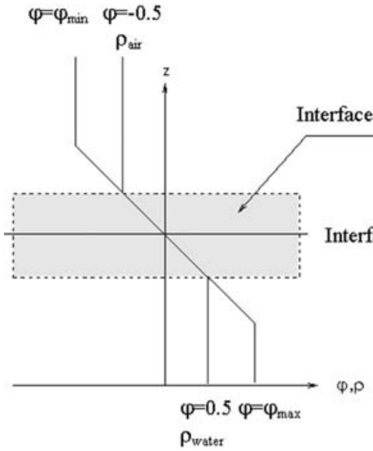

Fig. 1 Profiles of distance function and density

In general, the distance function is defined in a whole domain. However, there is a difficulty to set the boundary condition of the distance function on the outer boundary in satisfying the constant gradient of the distance function in the whole domain. In order to overcome the difficulty, the original level set method is modified in the present study.

Figure 1 shows the profile of distance function and density. The distance function is just defined near by the interface. The width of the interface band is limited two cells in the computation. The width of band where the distance function is not constant is slightly wider than the width of interface band. This definition is to use the reinitialization procedure of distance function. In outer region of interface band, the reinitialization is not necessary to keep the gradient of distance function because there is no gradient of the distance function in the regions. This is the way to overcome the difficulty of setting outer boundary condition for distance function. Uniform density is assumed in both the waterside and airside whereas a linear distribution of density is assumed in the interface band.

3.2 CIP method

The present study employs the CIP method by Yabe et al.(1991) which splits equation (1) into two stages, non-advection and advection assuming the time increment is infinitesimal.

In the non-advection stage, $\vec{v}^*$ can be calculated by equation (5).

$$\frac{\vec{v}^* - \vec{v}^m}{\Delta t} = -\frac{\nabla p^m}{\rho} + \frac{\mu}{\rho}\nabla^2 \vec{v}^m + \vec{F} \qquad (5)$$

where superscript * and m represent the time step in non-advection stage and Δt denotes the time increment. Pressure Poisson equation is derived from equation (5) by taking the divergence of both side.

$$\nabla\left(\frac{1}{\rho}\nabla p^*\right) = -\frac{\partial D^m}{\Delta t} + \nabla\left(\frac{\mu}{\rho}\nabla^2 \vec{v}^m + \vec{F}\right) \qquad (6)$$

where D is the divergence of velocity vector. Equations (5) and (6) are transformed into body fitted coordinates system and discretized by the finite difference method with the second order accuracy. The motion of equation in the advection stage including nonlinear term should be solved by a highly accurate numerical scheme. Once $\vec{v}^*$ and p^* are obtained in the non-advection stage, the CIP method, which can express the behavior of the solution inside two grid points, is applied to solve the flow advection. The function including the velocity components or distance function with its derivatives are expressed by the cubic polynomial in curvilinear coordinate system.

3.3 Modification of CIP method

The transport equation (3) is also calculated by the CIP method. As shown in Fig. 2, the numerical results for the transport equation demonstrate the coexistence of the numerical smearing and the overshooting for one-dimensional linear advection equation corresponding to different discretization schemes. The exactly identical initial shape of $f(x,t)$ for the analytic solution is plotted in Fig. 2. The initial profile shifts without variation of the shape.

The 3rd order upwind scheme and CIP method are used for the discretization of the advection and compared each other. Better solution is obtained by the CIP method rather than by the 3rd order upwind scheme. However, the overshooting is still observed in the result of the CIP method as shown in Fig. 3. The overshooting is prevented by a limit condition for the derivative of f as well

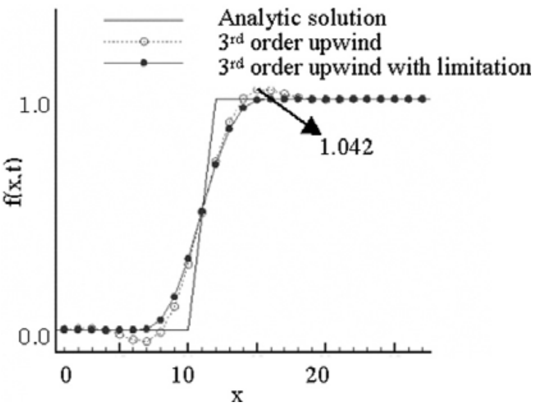

Fig. 2 Solution of 1-D advection equation by 3rd order upwind scheme

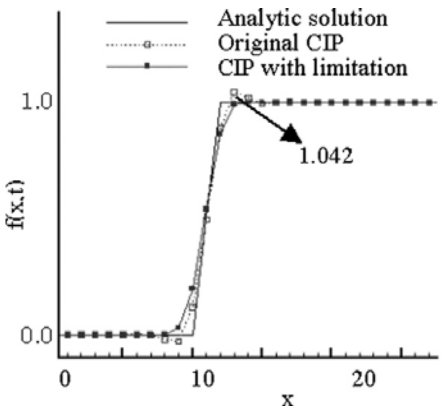

Fig. 3 Solution of 1-D advection equation by CIP method

as f itself. If f is greater than the upper maximum value or less than minimum value, the values are substituted by the maximum or minimum values and the derivative is also calculated again by the 3rd order upwind scheme. Unless the limit condition is carried out, an abnormal behavior may appear in the numerical result for the density. Even though the limit condition is adopted, it is found that the numerical smearing by CIP method is much less than that by the 3rd order upwind scheme. In the present study, the calculation of equation (3) is performed by the CIP method with the limit condition.

4. Results and Discussion

4.1 Examination of dependency of grid and free surface treatment

The dependency of grid system is checked by comparison between the computational results by the ITM and the experimental results for Wigley hull where Froude number based on ship length is 0.289 and Reynolds number is one million. To reduce the computational time, the free surface is traced by ITM. The minimum size of grid in each direction is determined by the ratio of fluid velocity component in each direction. The ratio of minimum grid size in both η and ζ direction is taken by 20 percent of the size in ξ direction. The maximum size of grid in each case is almost same each other. The number of grid points and the minimum grid size is shown in Table 1.

Table 1 Minimum Grid Size and number of grids

	Size (ξ)	Size (η)	Size (ζ)	No. of grids
Case 1	0.05L	0.01L	0.01L	26,460
Case 2	0.025L	0.005L	0.005L	49,700
Case 3	0.0125L	0.0025L	0.0025L	115,825
Case 4	0.00625L	0.00125L	0.00125L	229,908

Figure 4 exhibits the wave patterns according to the grid system. Because of the numerical damping, the wave pattern is not clear in far field in Case 1 and 2 whereas the wave patterns in Case 3 and 4 show distinct wave propagation. The comparison of wave elevation along the hull form is shown in Fig. 5. The wave elevation of Case 3 is very similar to that of Case 4. Through the observation of computed results, it is found that the grid resolution of Case 3 or Case 4 is appropriate for the evaluation of wave phenomena.

4.2 Comparison between Interface capturing and tracking method

The ICM should be adopted in the present study for the simulation of complex wave phenomena. The verification of ICM is performed by the comparison of wave patterns and elevations along hull surface. The computed wave elevations illustrated by Fig. 6 are very similar to the measured results. Also the wave pattern by ICM is similar to that of ITM as shown in Fig. 7. Through the comparison of wave elevation and pattern, it

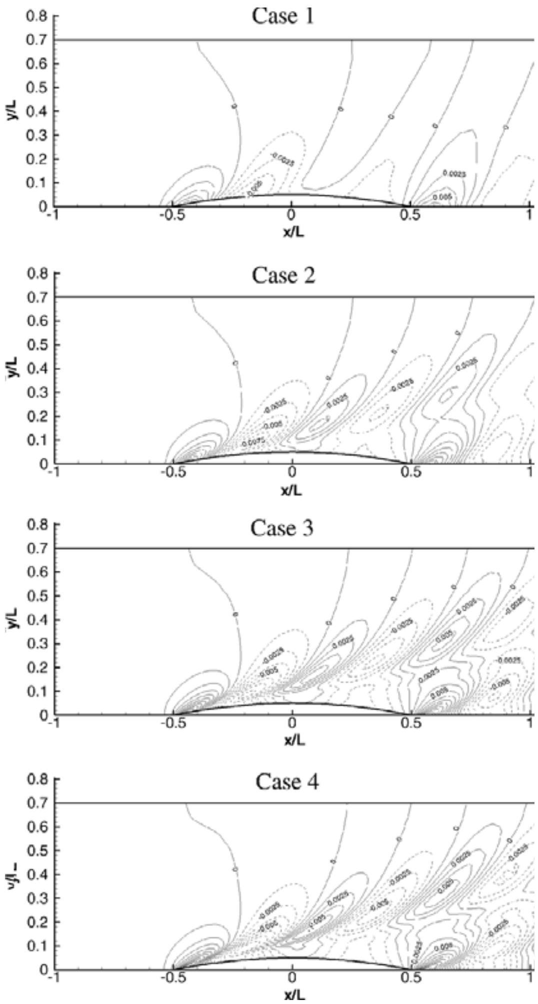

Fig. 4 Computed wave patterns by ITM

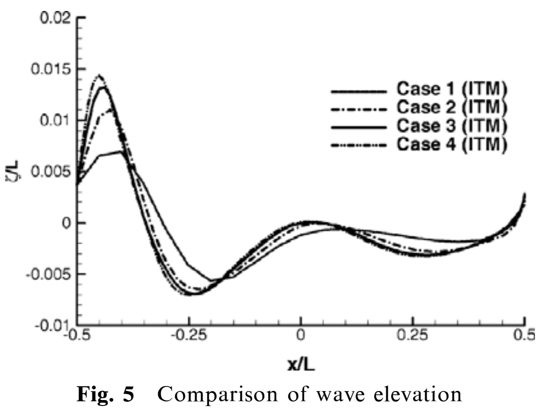

Fig. 5 Comparison of wave elevation

is found that the present numerical method is reliable way for the free surface simulation.

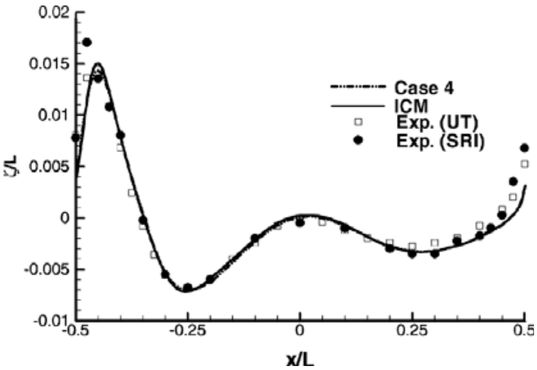

Fig. 6 Comparison wave elevation

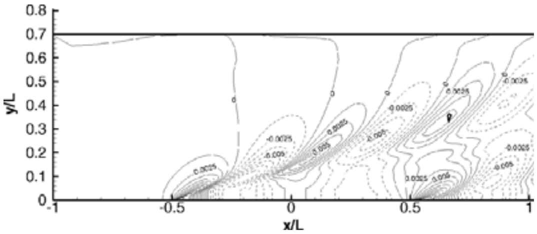

Fig. 7 Computed wave pattern by ICM

4.3 Application of numerical method to flow phenomena around Ro-Pax hull

The numerical method for the simulation of free surface flow around fast-ferry is applied to find the advantage of transom wedge. The grid quality is the same as that of Case 4 in the previous section. Fig. 8 shows the configuration of original transom and transom wedge whose chord length is 1% of ship length. The measured trim and sinkage of ship in the model test is used for those in the numerical simulation. The wave elevation at the rear part of transom was measured and the computed wave elevation is compared to the measured results as shown in Fig. 9. The relative wave height shows good agreement between computations and measurement. In addition, the spray phenomena are observed around 18 station in the computations and it is also confirmed by the observation of photograph shown in Fig. 10. It can be said that the present numerical method is applicable to the analysis of spray phenomena. Finally, pressure distribution and wave pattern are surveyed in order to discuss the improvement of resistance performance caused by transom wedge. In the comparison of positive pressure around

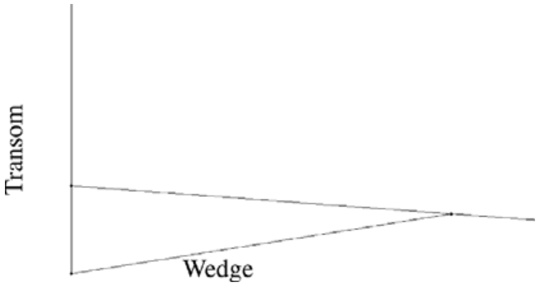

Fig. 8 Configuration of transom and wedge

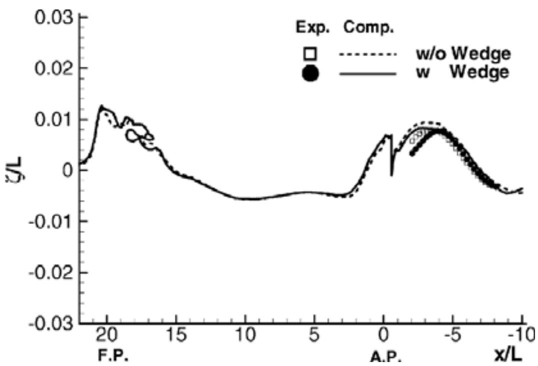

Fig. 9 Comparison of wave elevation

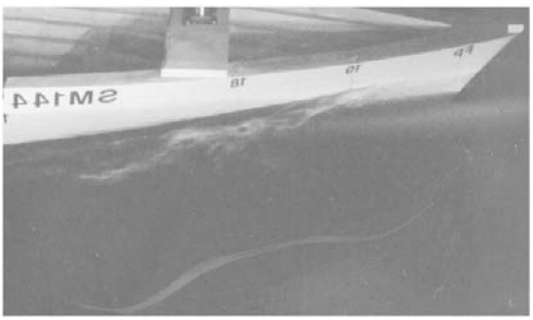

Fig. 10 Photograph of spray phenomenon

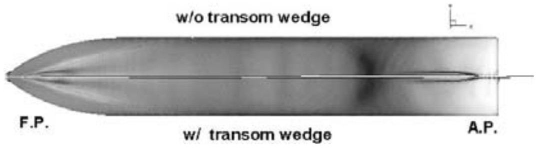

Fig. 11 Pressure distribution

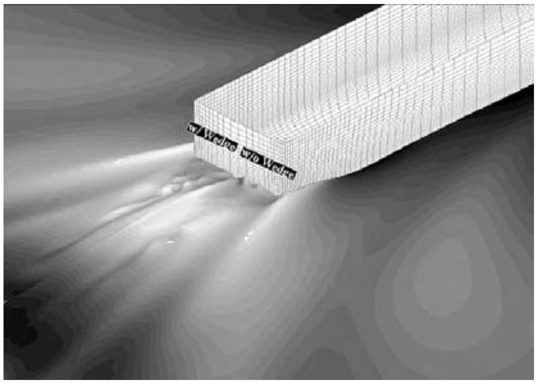

Fig. 12 Wave pattern around bare hull and hull with wedge

stern on bottom view, the magnitude of pressure on hull with transom wedge is greater than that of original as illustrated in Fig. 11. The improvement of transom wave system by the wedge is shown in Fig. 12. We can see that the wedge rectifies the transom flow through the comparison of wave patterns. From these it is expected that the pressure resistance and wave resistance of hull form with transom wedge is better than that of original. Also the improvement of resistance was confirmed by model test. The computed and measured pressure resistance coefficients of bare hull and hull with the wedge are listed in Table 2.

Table 2 Comparison of resistance coefficient between computation and experiment

	Computation (Pressure resistance coeff.)	Experiment (Residual resistance coeff.)
w/o wedge	2.52×10^{-3}	2.49×10^{-3}
w wedge	2.23×10^{-3}	2.26×10^{-3}

5. Conclusions

The level set method based on finite difference method is developed to simulate the complex free surface flow. The difficulty of original level set method is solved by the modification of profile of the distance function. The weak point of CIP method is also improved by the combination of 3rd order upwind scheme. The numerical method is validated by the comparison with measured data. Through the application of the numerical method for high-speed ship, it is found that the computed results by the present numerical method show good agreement with experiment. is Also it can be said that the transom wedge plays an important role in pressure recovery in stern resulting the resistance performance of hull with transom wedge becomes superior that of the original. As an additional finding, the numerical method can resolve the spray phenomena and the position of spray is predicted successfully.

References

Hong, C. B. and Lee, S. M., 2005, "Numerical Study on Characteristics of Ship Wave According to Shape of Waterway Section," *Journal of Mechanical Science and Technology*, Vol. 19, No. 12, pp. 2263～2269.

Karafiath, G., Cusanelli, D. S. and Lin, C. W., 1999, "Stern Wedges and Stern Flaps for Improved Powering — U.S. Navy Experience," *SNAME Annuel Meeting, Sept 1999. Baltimore, MD.*

Kong, F. Y., Lee, S. M. and Lee, Y. S., 2004, "Composite Overlapping Meshes for the Solution of Radiation force on Submerged-Plate," *KSME International Journal*, Vol. 18, No. 7, pp. 1203～1212.

Lee, S. M. and Hong, C. B., 2005, "Characteristics of Wave Exciting Forces on a Very Large Floating Structure with Submerged-Plate," *Journal of Mechanical Science and Technology*, Vol. 19, No. 11, pp. 2061～2067.

Miyata, H., Kajitani, H., Shirai, M., Sato, T., Kuzumi, S. and Kanai, M., 1985, "Numerical and Experimental Analysis of Monlinear Bow and Stern Waves of a Two-Dimensional Body (4^{th} report)-Siulation of Breaking Wave and Experimental Analysis," *Journal of the Society of Naval Architects of Japan*, Vol. 157, pp. 15～33.

Miyata, H., Katsumata, M., Lee, Y. G. and Kajitani, H., 1988, "A Finite-Difference Simulation Method for Strongly Interacting Two-Layer Flow," *Journal of the Society of Naval Architects of Japan*, Vol. 163, pp. 1～16.

Osher, S. and Sethian, J., 1988, "Front Propagating with Curvature Dependent Speed : Algorithm Based on Hamilton-Jacobi Formulations," *Journal of Computational Physics*, Vol. 79, pp. 12～49.

Sussman, M. and Fatemi, E., 1999, "An Efficient, Interface-Preserving Level Set Redistancing Algorithm and its Application to Interfacial Incompressible Fluid Flow," *SIAM Journal of Scientific Compute*, Vol. 20, No. 4, pp. 1165～1191.

Watanabe, Y. and Saeki, H., 1999, "Three-Dimensional Large Eddy Simulation of Breaking Waves," *Coastal Engineering Journal*, Vol. 41, pp. 281～301.

Yabe, T. and Wang, P. Y., 1991, "Unified Numerical Procedure for Compressible and Incompressible Fluid," *Journal of the Physical society of Japan*, Vol. 60, pp. 2105～2108.